NASA TECHNICAL NOTE

NASA TN D-3225
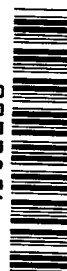
ANALYSIS OF FREE-MOLECULE FLOW WITH SURFACE DIFFUSION THROUGH CYLINDRICAL TUBES

by Thaine W. Reynolds and Edward A. Richley

Lewis Research Center
Cleveland, Ohio

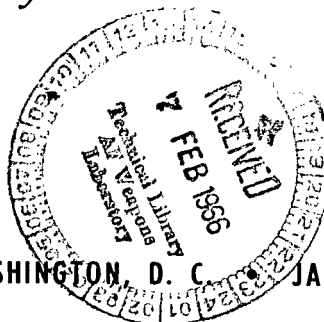NATIONAL AERONAUTICS AND SPACE ADMINISTRATION • WASHINGTON, D. C. • JANUARY 1966

ANALYSIS OF FREE-MOLECULE FLOW WITH SURFACE

DIFFUSION THROUGH CYLINDRICAL TUBES

By Thaine W. Reynolds and Edward A. Richley

Lewis Research Center
Cleveland, Ohio

NATIONAL AERONAUTICS AND SPACE ADMINISTRATION

ANALYSIS OF FREE-MOLECULE FLOW WITH SURFACE

DIFFUSION THROUGH CYLINDRICAL TUBES

by Thaine W. Reynolds and Edward A. Richley

Lewis Research Center

SUMMARY

The integrodifferential equation governing flow through cylindrical tubes under combined free-molecule gas flow and surface diffusion has been solved numerically for tube length-to-radius ratios of 1/16, 1/8, 1, 4, and 16 and for a wide range of flow parameters. Several transmission probability relations are developed that permit various comparisons of flow with and without surface diffusion for given tube length-to-radius ratios. General results are tabulated for inlet and outlet surface coverage fractions, gradients in surface coverage fraction, and transmission factors.

Specific solutions for tube flows matched to inlet and outlet surface flows are given. Results are presented for the single tube solutions only, but relations are given by which these results can be applied to models of porous media as well. In the matched solutions, the total transmission factor increased with increasing values of the surface diffusion parameter. The solutions are shown to be asymptotic to the long tube approximations.

Results are compared with those of other investigators and differences are found to be primarily due to variations in basic assumptions with respect to the model.

INTRODUCTION

Flow of gases at low pressures through tubes of small diameter (of the order of microns) may be influenced considerably by the process of surface diffusion of adsorbed molecules along the walls of the passage. These surface diffusion effects have been of concern in the evaluation of the flow through small single tubes (or orifices) such as utilized in the Knudsen cell measurements of vapor pressure (ref. 1), as well as in the study of flow through various porous media. Examples of the latter include powder beds for gas adsorption (ref. 2), porous plugs for cathodes (ref. 3), and certain ion rockets (refs. 4 and 5). The theoretical approach to treatment of these flows is usually a single tube model.

Free-molecule flow of gases (i.e., flow at very low pressures) through passages of various cross sections appears to be adequately treated (refs. 3, 6, 7, and 8); however, the combined mechanism of free-molecule and surface diffusion flow has received much less attention. Usually, efforts to solve the combined flow problem are directed toward specific applications (e.g., refs. 1, 5, 9, and 10). The resulting solutions are often restricted to a particular system (i.e., to a specific configuration or to a specific gas-metal combination) because of the boundary conditions and simplifying assumptions that were made. For example, the orifice flow treatment in reference 1 is restricted to length-to-radius ratio tubes much less than unity. Treatments such as described in references 9 and 10 are restricted to long tubes (length-to-radius ratio >50) because of the use of the limiting form of the Clausing factor and other restricting assumptions. The analysis presented in this report, is not restricted in length-to-radius ratio, but covers the range from zero to lengths where the long tube approximations become applicable.

The problem is such that more than one equation may be required to describe the flow; for example, one for flow through the tube, one for flow along the upstream surface, and one for flow along the downstream surface (see sketch (a)). The equation describing the combined free-molecule and surface-diffusion flow through the tube is the most complex. It is a second-order integrodifferential equation not amenable to closed-form solution. Various boundary conditions may be specified, which in turn must be matched to conditions at the inlet and exit ends of the tube to obtain a complete solution. These boundary conditions will be discussed in detail in terms of the physical requirements of the problem. Transmission coefficients for the combined flow are also developed and presented.

An important feature of the tube flow solutions presented herein is that they are obtained by an iterative numerical method that exhibits very rapid convergence and is completely general. The technique is described in appendix D by Carl D. Bogart.

ANALYSIS

The Model

Establishing an appropriate mathematical model from the physical one appears extremely difficult if all possible aspects are to be included, that is, if it is to represent a pore in a piece of porous material as well as a simple cylindrical hole in a plate. In the former case, where gross flow characteristics are primarily of interest, recourse is often made to the inclusion of uncertainty factors applied to macroscopic flow relations without regard for the detailed physical model (ref. 2). These factors must then be evaluated experimentally for specific systems. Another macroscopic approach (described in detail in ref. 4) treats the porous medium as if it consisted of parallel capillaries having some mean capillary radius. Physically this model also seems to be satisfactory for a microscopic approach as long as it is recognized as merely a convenient tool for mathematical analysis. The analysis can be constructed around a single typical capillary, and it is equally applicable to a wide variety of problems. The model used herein is depicted in sketch (a), which shows the

2

End view

Cross section through single capillary
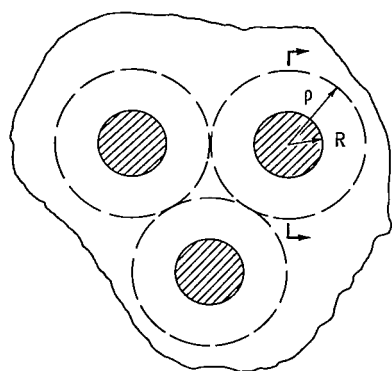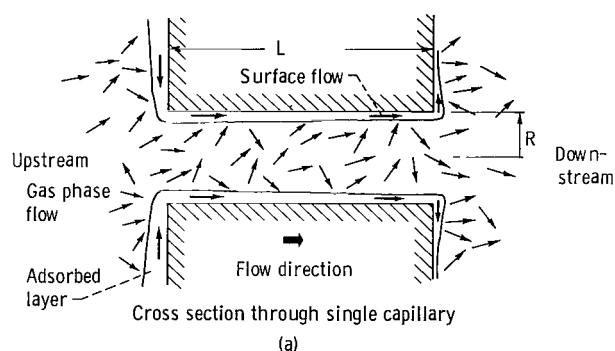
(a)

gas-phase and surface-diffusion compo-
nents of the flow. Throughout this
report the use of the term gas-phase
is restricted to mean that component
of particle flow in free space and
does not include any particle flow
along surfaces. That flow which in-
cludes both components will always
have the term total attached to it.

Ahead of the upstream end of the
tube, the gas is in equilibrium. Par-
ticles arrive at and evaporate from
the wall leaving it with a net surface
coverage. Because of surface diffu-
sion, the surface coverage is shown to
decrease along the upstream surface in
the direction of the tube entrance.
Surface-diffusion flow takes place
through the tube also, and in this
case there is an accompanying gas-
phase flow. The gas-phase flow is
assumed to be free-molecule flow; that
is, particle-particle collisions are
negligible and only particle-wall col-
lisions must be considered. Along the
downstream surface, which is exposed
to vacuum, flow is by surface diffu-
sion with evaporation. Thus, it can
be seen that the system can be broken into three segments. These segments will
be described in detail in the next section and the governing mathematical rela-
tions will be developed. Additional appropriate assumptions or restrictions
regarding the flow will be introduced as they become applicable.

The Tube

Flow through the tube consists of both gas-phase and surface-diffusion
flow. Particles arrive at and depart from the tube wall in much the same way
that takes place on the upstream surface; however, as will be seen, the mathe-
matical relation describing the process differs considerably. Particle leaving
rate from the tube wall when no surface-diffusion effect is considered is given
by the following equation first derived by Clausing (ref. 6) and developed in
detail in reference 8:

$$\nu(\bar{x}_2) = \mu_1 F_{1,2} + \int_0^{\bar{L}} \nu(\bar{x}) F_{3,2} \, d\bar{x} \tag{1}$$

(Symbols are defined in appendix A.) The barred quantities are dimensionless
ratios with respect to the tube radius R. Sketch (b) will aid in visualizing
the physical significance of the terms in equation (1).
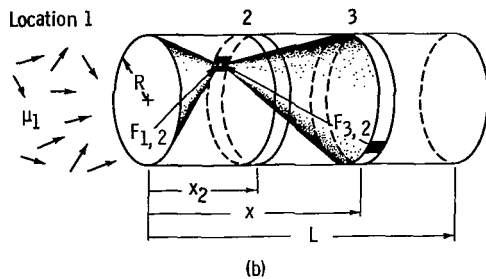
The left side of equation (1) is the local net leaving rate at an element of area at location 2 and is assumed equal to the local net arrival rate. On the right side of the equation, the term $\mu_1 F_{1,2}$ is the arrival rate of particles directly from the inlet. The quantity $F_{1,2}$ is a geometric factor arising from the assumption that the flow has a random directional distribution (ref. 8):

$$F_{1,2} = \frac{1}{2}\left[\frac{\overline{x}_2^2 + 2}{(\overline{x}_2^2 + 4)^{1/2}} - \overline{x}_2\right] \qquad (2)$$

The second term on the right side of equation (1) is the arrival rate of particles from the tube wall (location 3) integrated over the complete area of the wall. It will be recognized that $\nu(\overline{x})$ is the function of which $\nu(\overline{x}_2)$ is a local value. The geometric factor in this term is

$$F_{3,2} = \frac{1}{2}\left\{1 - |\overline{x} - \overline{x}_2|\,\frac{(\overline{x} - \overline{x}_2)^2 + 6}{[(\overline{x} - \overline{x}_2)^2 + 4]^{3/2}}\right\} \qquad (3)$$

An analytic solution to equation (1) has not yet been published; however, numerical solutions have been obtained by several investigators (refs. 8, 11 to 19). The results show that $\nu(\overline{x})$ is almost linear. An interesting feature of this near linear relation is discussed in appendix B.

If an adsorbed layer is present on the tube walls, then a term accounting for surface-diffusion flow must be added to equation (1):

$$\nu(\overline{x}_2) = \mu_1 F_{1,2} + \int_0^{\overline{L}} \nu(\overline{x})F_{3,2}\,d\overline{x} + \frac{\mathscr{D}}{R^2}\sigma''(\overline{x}_2) \qquad (4)$$

This added term represents the net accumulation of particles at location 2 due to flow by surface diffusion. It is the solution of equation (4) that is of primary interest to describe the flow through the tube. (A derivation of eq. (4) is given in ref. 3.) Before a solution of equation (4) can be attempted, a relation between the local leaving rate ν and surface concentration σ is required. Where experimental data are available for a specific system they may be used (see ref. 5). More generally, various analytical relations for surfaces at constant temperature (adsorption isotherms) have been developed and are given in the literature. A detailed discussion of all these is beyond the scope of this report; however, appendix C is included to give an insight into some of the fundamental assumptions and common relations. As discussed in appendix C, the relation used herein, which is also an appropriate approximation of all the relations given, for low values of surface coverage fraction $\theta(\theta = \sigma/\sigma_m)$, is

4

$$\nu = \frac{\sigma}{\tau} = \frac{\sigma_m \theta}{\tau} = C_1 \theta \tag{5}$$

A useful concept is the time required to deposit a monolayer onto a clean surface assuming no evaporation occurs:

$$\tau_m = \frac{\sigma_m}{\mu_1} \tag{6}$$

Then, when the evaporation rate ν equals the arrival rate μ_1, the surface coverage fraction can be designated (from eqs. (5) and (6)) as

$$\theta_\infty = \frac{\sigma_1}{\sigma_m} = \frac{\tau}{\tau_m} \tag{7}$$

The surface coverage fraction θ_∞ is the maximum value of coverage that is expected in any system in the sense that it is at the maximum arrival rate and occurs in the absence of surface diffusion effects. Then, at any other evaporation rate $\nu(\bar{x})$, again from equations (5) and (6),

$$\frac{\nu(\bar{x})}{\mu_1} = \frac{\sigma}{\tau} \frac{\tau_m}{\sigma_m} = \frac{\dfrac{\sigma}{\sigma_m}}{\dfrac{\tau}{\tau_m}} = \frac{\theta(\bar{x})}{\theta_\infty} \tag{8}$$

Thus, by using equation (8), equation (4) can be expressed in terms of θ as

$$\bar{\theta}(\bar{x}_2) = F_{1,2} + \int_0^{\bar{L}} \bar{\theta}(\bar{x}) F_{3,2} \, d\bar{x} + C_2 \bar{\theta}''(\bar{x}_2) \tag{9}$$

where

$$\bar{\theta}(\bar{x}) = \frac{\theta(\bar{x})}{\theta_\infty} \tag{10}$$

and

$$C_2 = \frac{\mathscr{D} \sigma_m}{\mu_1 R^2} \theta_\infty \tag{11}$$

With the specification of C_2, $\bar{L}$ and two boundary conditions, equation (9) can be solved by using iterative numerical techniques. The required boundary conditions can be specified by selecting any two of the variables $\bar{\theta}(0)$, $\bar{\theta}(\bar{L})$, $\bar{\theta}'(0)$, or $\bar{\theta}'(\bar{L})$. The choice is a matter of convenience with respect to the particular numerical procedure used. In the one used herein the values of $\bar{\theta}(0)$ and $\bar{\theta}(\bar{L})$ are specified as boundary conditions (see appendix D). Values

(c)
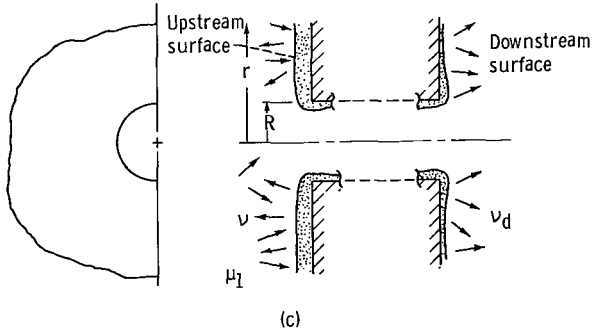
of $\bar{\theta}'$ (needed later) are then obtainable from the resulting solutions.

Mathematical solutions of equation (9) may be obtained without regard for upstream surface or downstream surface flows. As will be seen however, depending on the physical model of the system, only certain of the solutions may be applicable.

The Upstream and Downstream Surfaces

For the model chosen as illustrative of one physical system the upstream and downstream surfaces may be regarded as annular surfaces of inner radius R, as shown in sketch (c).

Upstream surface. - The differential equation describing the steady-state surface concentration σ is (ref. 5)

$$\mathscr{D}\left[\sigma''(\bar{r}) + \frac{1}{\bar{r}} \sigma'(\bar{r})\right] = R^2(\nu - \mu_1) \tag{12}$$

Equation (12) can be rewritten by using equations (5) and (11) as

$$\bar{r}^2\bar{\theta}''(\bar{r}) + \bar{r}\bar{\theta}'(\bar{r}) - \bar{r}^2 C_3\bar{\theta} = -C_3\bar{r}^2 \tag{13}$$

where

$$C_3 = \frac{R^2}{\mathscr{D}\tau} = \frac{1}{C_2} \tag{14}$$

from equations (6), (7), and (11).

Equation (13) is in the form of a modified Bessel equation for which the general solution is

$$\bar{\theta}(\bar{r}) = bI_0(\bar{r}\sqrt{C_3}) + cK_0(\bar{r}\sqrt{C_3}) + 1 \tag{15}$$

For a single tube or hole in a plate, as $\bar{r}$ gets large, $\theta(\bar{r})$ approaches θ_∞. This requires the constant b to be zero since I_0 goes to infinity and K_0 goes to zero with increasing $\bar{r}$. For this case

$$\bar{\theta}(\bar{r}) = cK_0(\bar{r}\sqrt{C_3}) + 1 \tag{16}$$

In general, however, for closely spaced tubes (pores) the constant b is not zero. Assume that at some maximum radial distance $\bar{\rho}$ the concentration gradient is zero; that is,

6

$$\bar{\theta}'(\bar{\rho}) = 0 \tag{17}$$

Applying this boundary condition to equation (15) yields

$$\frac{b}{c} = \frac{K_1(\bar{\rho}\sqrt{C_3})}{I_1(\bar{\rho}\sqrt{C_3})} \tag{18}$$

By using this relation, then, equation (15) becomes for the general case

$$\frac{1 - \bar{\theta}(\bar{r})}{1 - \bar{\theta}_R} = \frac{\dfrac{K_1(\bar{\rho}\sqrt{C_3})}{I_1(\bar{\rho}\sqrt{C_3})} I_0(\bar{r}\sqrt{C_3}) + K_0(\bar{r}\sqrt{C_3})}{\dfrac{K_1(\bar{\rho}\sqrt{C_3})}{I_1(\bar{\rho}\sqrt{C_3})} I_0(\sqrt{C_3}) + K_0(\sqrt{C_3})} \tag{19}$$

For widely spaced pores this reduces to the single tube relation (i.e., for $\bar{\rho} \to \infty$),

$$\frac{1 - \bar{\theta}(\bar{r})}{1 - \bar{\theta}_R} = \frac{K_0(\bar{r}\sqrt{C_3})}{K_0(\sqrt{C_3})} \tag{20}$$

Differentiation of equation (19) yields for the slope

$$\bar{\theta}'(\bar{r}) = -(1 - \bar{\theta}_R)\sqrt{C_3}\; \frac{\dfrac{K_1(\bar{\rho}\sqrt{C_3})}{I_1(\bar{\rho}\sqrt{C_3})} I_1(\bar{r}\sqrt{C_3} - K_1(\bar{r}\sqrt{C_3})}{\dfrac{K_1(\bar{\rho}\sqrt{C_3})}{I_1(\bar{\rho}\sqrt{C_3})} I_0(\sqrt{C_3}) + K_0(\sqrt{C_3})} \tag{21}$$

which for the single tube at $\bar{r} = \bar{R}$ becomes

$$\bar{\theta}_R' = (1 - \bar{\theta}_R)\sqrt{C_3}\; \frac{K_1(\sqrt{C_3})}{K_0(\sqrt{C_3})} \tag{22}$$

With C_3 specified equation (22) may be solved for various values of $\bar{\theta}_R$. This equation will be considered in detail in the section Matched Boundary Solutions.

The quantities θ_∞ and C_3 are not independent but are related from equations (7) and (14):

$$C_3 = R^2(\mathscr{D}\theta_\infty \tau_m)^{-1} \tag{23}$$

Downstream surface. - There is no gas-phase arrival rate on the downstream surface (see sketch (c)), and the differential equation describing the steady-

state surface concentration on this surface is

$$\mathcal{D}\left[\sigma''(\bar{r}) + \frac{1}{\bar{r}}\,\sigma'(\bar{r})\right] = \nu_d R^2 \tag{24}$$

A development similar to that used for the upstream surface leads to the following solutions:

For the general case of closely spaced pores

$$\frac{\bar{\theta}(\bar{r})}{\bar{\theta}_R} = \frac{\dfrac{K_1(\bar{\rho}\sqrt{C_3})}{I_1(\bar{\rho}\sqrt{C_3})}\,I_0(\bar{r}\sqrt{C_3}) + K_0(\bar{r}\sqrt{C_3})}{\dfrac{K_1(\bar{\rho}\sqrt{C_3})}{I_1(\bar{\rho}\sqrt{C_3})}\,I_0(\sqrt{C_3}) + K_0(\sqrt{C_3})} \tag{25}$$

and for the single tube or pore

$$\frac{\bar{\theta}(\bar{r})}{\bar{\theta}_R} = \frac{K_0(\bar{r}\sqrt{C_3})}{K_0(\sqrt{C_3})} \tag{26}$$

The slope for the general case is

$$\bar{\theta}'(\bar{r}) = \bar{\theta}_R\sqrt{C_3}\,\frac{\dfrac{K_1(\bar{\rho}\sqrt{C_3})}{I_1(\bar{\rho}\sqrt{C_3})}\,I_1(\bar{r}\sqrt{C_3}) - K_1(\bar{r}\sqrt{C_3})}{\dfrac{K_1(\bar{\rho}\sqrt{C_3})}{I_1(\bar{\rho}\sqrt{C_3})}\,I_0(\sqrt{C_3}) + K_0(\sqrt{C_3})} \tag{27}$$

and for the single tube at $\bar{r} = \bar{R}$

$$\bar{\theta}_R' = -\bar{\theta}_R\sqrt{C_3}\,\frac{K_1(\sqrt{C_3})}{K_0(\sqrt{C_3})} \tag{28}$$

With C_3 specified equation (28) may be solved for various values of $\bar{\theta}_R$. This equation will be considered in detail in the section Matched Boundary Solutions.

The similarity between the upstream and downstream relations is apparent. Figure 1 is a plot of the specified functions that appear in both equations (21) and (27). This combination of functions is herein defined as

8

$$\mathscr{F}(C_2) = \sqrt{C_3} \; \frac{\dfrac{K_1(\overline{\rho}\sqrt{C_3})}{I_1(\overline{\rho}\sqrt{C_3})} I_1(\overline{r}\sqrt{C_3}) - K_1(\overline{r}\sqrt{C_3})}{\dfrac{K_1(\overline{\rho}\sqrt{C_3})}{I_1(\overline{\rho}\sqrt{C_3})} I_0(\sqrt{C_3}) + K_0(\sqrt{C_3})} \tag{29}$$

and is plotted against the variable C_2 in figure 1, C_2 being the reciprocal of C_3 (eq. (14)).

It is apparent from figure 1 that for values of C_2 less than about unity, the $\overline{\theta}'$ solutions for the single tube case ($\overline{\rho} = \infty$) are applicable to closely spaced pores ($\overline{\rho} \approx 2$) as well. Subsequent solutions will be presented only for the case $\overline{\rho} = \infty$. The solutions for cases of $\overline{\rho}$ less than infinity may be obtained by following the same procedures to be outlined for the single tube case, but by using the appropriate curve from figure 1.

Matching Boundary Conditions

Three equations of primary interest for the physical model are equation (9) describing the tube flow, equation (21) describing the upstream surface flow, and equation (27) describing the downstream surface flow. These equations are mathematically independent in that each may be solved with no knowledge of the others. The resulting solutions may be combined to represent a physical system provided some interrelation is specified.

In the treatment of the physical model given herein, complete solutions that satisfy the following boundary conditions will be presented:

$$\theta_0 = \theta_R \text{ (upstream)} \tag{30a}$$

$$\theta'_0 = \theta'_R \text{ (upstream)} \tag{30b}$$

$$\theta_L = \theta_R \text{ (downstream)} \tag{30c}$$

$$\theta'_L = \theta'_R \text{ (downstream)} \tag{30d}$$

In addition, a wide variety of independent tube flow solutions will be given from which it is possible to construct complete solutions to other physical systems.

The same boundary conditions (eqs. (30a) to (30d)) are specified in reference 5. In reference 1, θ_R at the upstream end is equated to θ_∞, thus eliminating all upstream surface diffusion effects from the system. At the downstream end the required matching condition of reference 1 is the same as equation (30d).

9

Surface-
diffusion
flow, n_2

Gas-phase
flow, n_1

n_4

n_3

Inlet
plane,
x = 0

Exit
plane,
x = L

(d)
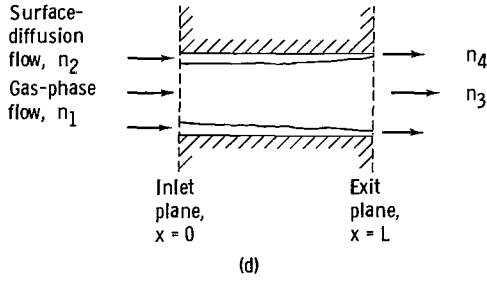
The various transmission factors that are defined in the case of gas-phase transport alone are all ratios of the net flow out the exit to the inlet gas-phase arrival rate. For that case there is no other flow mechanism introducing material into the tube; however, with surface transport possible, as in the present case, some mass flow may be introduced into the tube by surface transport also. It may, in fact, exceed that introduced by the gas-phase transport. Nevertheless, it is still convenient to define transmission factors based on the inlet gas-phase arrival rate alone, even though the transmission factor may then exceed unity. The inlet gas arrival rate is a readily evaluated number, independent of the tube flow conditions, while the surface transport portion of the inlet flow is not. The various transmission factors presented herein, therefore, are all referred to the inlet gas arrival rate only.

Consider the system depicted in sketch (d). The mass flow (particles/sec) crossing the inlet plane due to gas-phase flow is

$$n_1 = \mu_1 \pi R^2 \tag{31}$$

and that due to surface-diffusion flow is

$$n_2 = -2\pi R \mathscr{D} \left(\frac{d\sigma}{dx} \right)_0 = -2\pi \mathscr{D} \sigma_m \theta'_0 \tag{32}$$

At the exit plane the mass flow expressions are more complex. The gas-phase flow is

$$n_3 = P_G \mu_1 \pi R^2 \tag{33}$$

where P_G is a gas-phase transmission factor, defined as the ratio of the gas-phase flow passing the outlet plane to the gas-phase flow entering across the inlet plane. As shown in reference 8, P_G may be considered to consist of two components, a direct and an indirect transmission factor:

$$P_G = P_d + P_i \tag{34}$$

where P_d is simply the fraction of entering particles that pass directly through the tube without any encounters with the wall. It is a function only of $\bar{L}$:

$$P_d = 1 + \frac{\bar{L}^2}{2} - \frac{\bar{L}}{2} \sqrt{(\bar{L}^2 + 4)} \tag{35}$$

The flow P_i is the ratio of the exiting gas-phase flow coming off the tube wall to the entering gas-phase flow. It is given by the following integral (ref. 8):

$$P_i = 4 \int_0^1 \overline{r} \int_0^{\overline{L}} \overline{\theta}(\overline{x}) \frac{(\overline{L} - \overline{x})\left[(\overline{L} - \overline{x})^2 + 1 - \overline{r}^2\right]}{\left\{\left[(\overline{L} - \overline{x})^2 + 1 + \overline{r}^2\right]^2 - 4\overline{r}^2\right\}^{3/2}} d\overline{x}\, d\overline{r} \tag{36}$$

The function $\overline{\theta}(\overline{x})$ is given by equation (9).

The surface-diffusion flow out the exit is

$$n_4 = -2\pi R \mathscr{D} \left(\frac{d\sigma}{dx}\right)_L = -2\pi \mathscr{D} \sigma_m \theta_L' \tag{37}$$

The total transmission factor is, then,

$$P_T = \frac{n_3 + n_4}{n_1} = P_G + P_S \tag{38}$$

where P_S is a newly defined surface transmission factor

$$P_S = \frac{n_4}{n_1} = -2C_2 \overline{\theta}_L' \tag{39}$$

Other Considerations

General numerical solutions of the tube flow equation (eq. (9)) are obtainable with the specification of C_2, $\overline{L}$, $\overline{\theta}_0$, and $\overline{\theta}_L$. Since solutions are obtained by an iterative procedure, specification of a convergence factor ϵ is also required. Convergence is defined herein in terms of this factor as

$$\left|\frac{\overline{\theta}(\overline{x})_{n+1} - \overline{\theta}(\overline{x})_n}{\overline{\theta}(\overline{x})_n}\right|_{max} < \epsilon \equiv 10^{-5} \tag{40}$$

Before going on to the general and matched-boundary solutions, a brief discussion on the makeup of the θ_∞ and C_2 terms may aid in considering the physical interpretation of the results. As seen from equation (7), specifying θ_∞ from physical considerations requires a knowledge of the upstream equilibrium arrival rate μ_1 and the parameter C_1. For a given gas μ_1 is related to the pressure and temperature:

$$\mu_1 = p(2\pi MkT)^{-1/2} \tag{41}$$

As an example, figure 2 is included to show the variation of μ_1 with T for a few substances, where the vapor pressure relations of p with T from reference 20 have been used. The parameter C_1 is expressed in terms of the quantities σ_m, γ, τ_0, Q, and T_{eV} from equation (C10). Some of these are

11

fairly constant, but others are highly uncertain and may vary widely with material. For many materials the monolayer coverage σ_m is on the order of 10^{15} atoms per centimeter squared. As mentioned in appendix C, the sticking coefficient γ has been assumed to be unity. The quantity τ_0 is a proportionality constant relating the mean adsorption lifetime τ with the desorption energy Q and the temperature of the system (eq. (C7)). A reasonable value of τ_0 is about 10^{-13} second although values considerably larger than this have been reported. Based on the value of 10^{-13}, figure 3 gives the variation of $\log_{10}\tau$ with Q for various values of T. If the relation between Q and T is known for a given system, all the quantities necessary for evaluating θ_∞ are available.

As shown in equation (11), two additional parameters are required to evaluate C_2: the surface-diffusion coefficient $\mathscr{D}$ and the tube radius R. Experimental values of $\mathscr{D}$ are very sparse. A value of 10^{-4} centimeter squared per second was assumed for silver vapor on molybdenum and on nickel in reference 1. At high temperature the value of $\mathscr{D}$ for cesium on tungsten is also about 10^{-4} centimeter squared per second (ref. 21). A theoretical approach to describing $\mathscr{D}$ is also given in reference 21, where $\mathscr{D}$ is considered to depend upon the adsorption time τ and the mean transit time t. The relation employed is

$$\mathscr{D} = \frac{1}{4}\frac{a^2}{\tau + t} \tag{42}$$

where the mean transit time across an adsorption site t is

$$t = \frac{a}{v} = \frac{a}{\left(\dfrac{\pi k T}{2m}\right)^{1/2}} \tag{43}$$

At low temperature the adsorption time is much longer than the transit time, and $\mathscr{D}$ exhibits an exponential temperature dependence. At high temperature the transit time becomes controlling, and then $\mathscr{D}$ varies as the square root of the temperature. This behavior is portrayed in sketch (e). At the higher temperature levels then, it is reasonable to expect $\mathscr{D}$ to be of the same order of magnitude for different systems, its variation being only inverse with the square root of the particle mass. The use of the term high temperature is only relative, of course, the important factor being the relation of the adsorption and transit times.

This in brief describes the physical parameters of interest. It should also be pointed out that with regard to the upstream and downstream surface flow relations, (eqs. (21) and (27)), no additional parameters are required to define C_3.

The following sketch recapitulates the material discussed thus far. In sketch (f) the circled numbers refer to applicable equations, and the relation of p and Q to T is assumed known. As pointed out previously, specification of certain physical parameters imposes interrelations among the C's (e.g., eq. (23)). Conversely, the C's may be specified with no knowledge of the physical parameters.

12

(e)

(f)
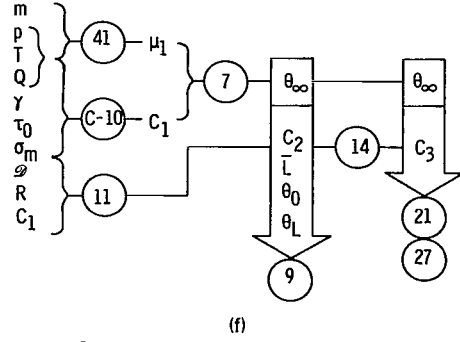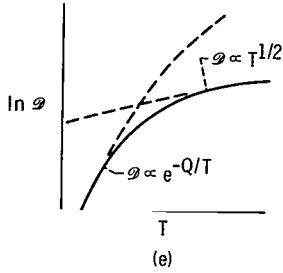
RESULTS AND DISCUSSION

General Tube Solutions

Solutions to equation (9) were carried out on an IBM 7094 computer by using the procedure outlined in appendix D. Initially, solutions were obtained for various pairs of $\bar{\theta}_0$, $\bar{\theta}_L$ values for each combination of $\bar{L}$ and C_2. It is not practical to present all the tube-wall coverage data that were obtained. Sketches (g), (h), and (i) are shown as typical examples for various levels of coverage at the end points. The trend of the solutions which was obtained in all cases can be noted from these sketches. When $\bar{\theta}_0$ and $\bar{\theta}_L$ are fixed, the

(g)

(h)

(i)

(j)

(k)

(l)
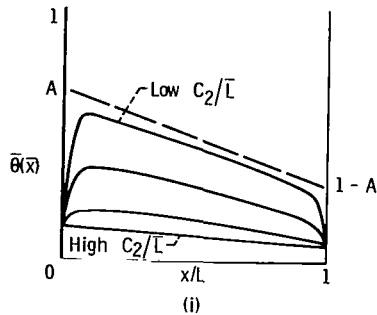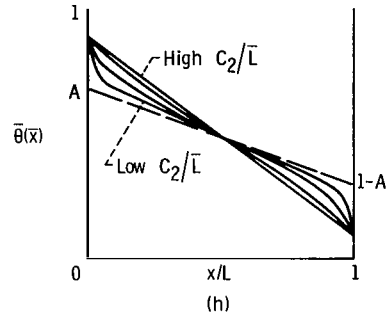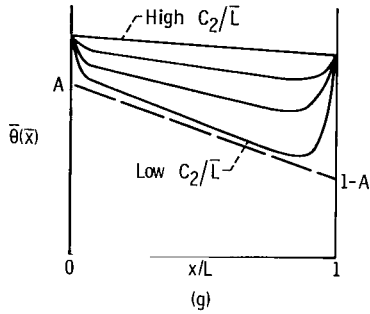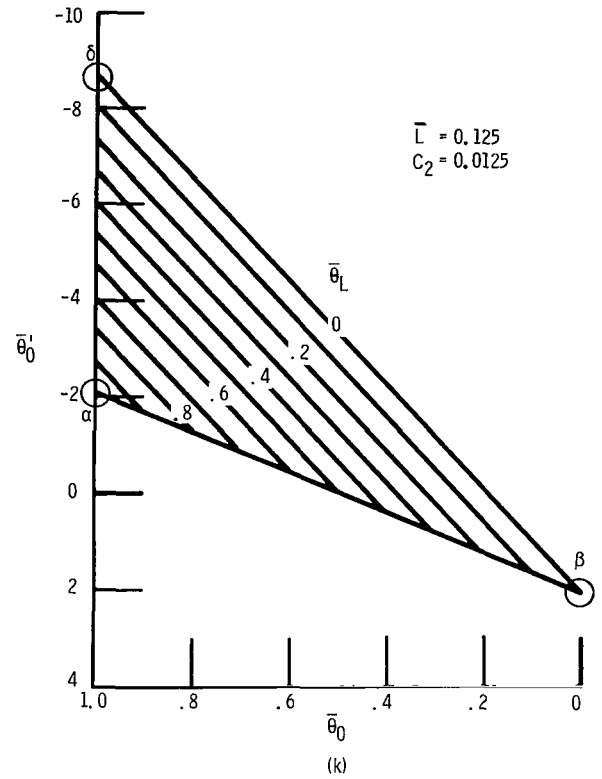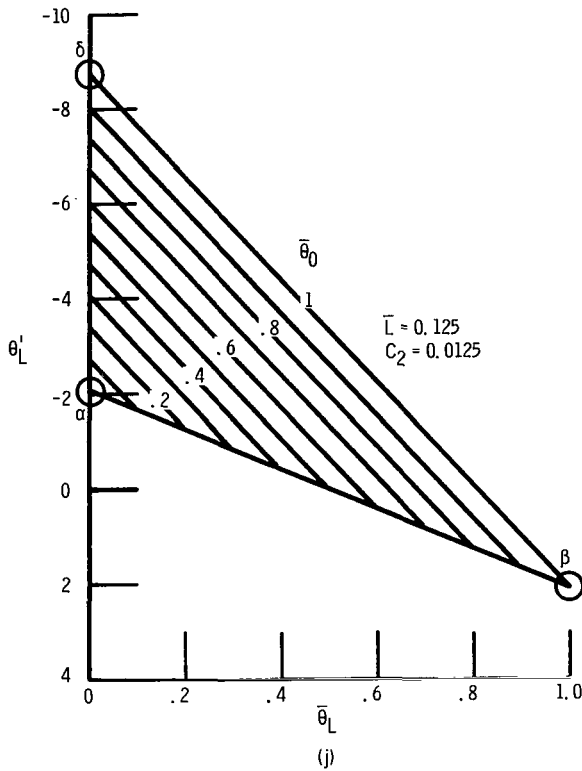
solution varies from a straight line through $\bar{\theta}_0$ and $\bar{\theta}_L$ at high $C_2/\bar{L}$ values, and tends toward the straight line through A and 1 - A as $C_2/\bar{L}$ approaches zero (see appendix B), except for holding to the imposed end-point values.
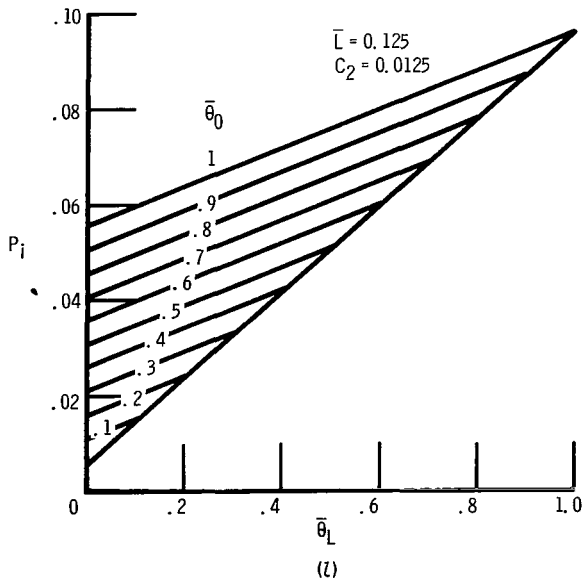
From various plots of the solutions, it was found that all values of $\bar{\theta}_0'$, $\bar{\theta}_L'$, and P_i could be represented by "maps" as shown in sketches (j), (k), and (l). These maps can be constructed from three sets of $\bar{\theta}_0$, $\bar{\theta}_L$ conditions. These latter results are summarized in tables I and II. Table I has values of the slopes $\bar{\theta}_0'$ and $\bar{\theta}_L'$ for the combinations, (a) $\bar{\theta}_0 = 1.0$, $\bar{\theta}_L = 1.0$; (b) $\bar{\theta}_L = 1.0$, $\bar{\theta}_0 = 0$; and (c) $\bar{\theta}_0 = 0$, $\bar{\theta}_L = 0$. Table II contains values of the indirect transmission factors P_i for the same sets of parameters.

14

The three values for each $C_2/\overline{L}$ that are given in the tables can be used to map the solutions for any set of end-point conditions as indicated in sketches (j), (k), and (l). These 3 points in table I are designated α, β, and δ to assist in showing their use in constructing the solution maps. Note that the graphs of sketches (j) and (k) are identical when the coordinates are labeled in the manner illustrated.

The gas-phase transmission factor P_G (eq. (34)) differs from P_i only by the factor P_d and is not tabulated. The direct-transmission probability P_d is only a function of $\overline{L}$ (eq. (35)) and is shown plotted in figure 4. Similarly, the surface-diffusion transmission factor P_S is readily obtainable from the tabulated values of slope $\overline{\theta}_L'$ through equation (39) and thus is not tabulated. It will be noted in sketches (g) and (h) that for a given $\overline{L}$ as C_2 decreases, the absolute magnitude of the slopes at the end points increases; however, the product $C_2\overline{\theta}'$, which is a factor in the surface-diffusion flow transmission factor, decreases as C_2 decreases, as would be expected.

<div align="center">Matched Boundary Solutions</div>

The matched tube and end-plate solutions are readily obtained by using the graphs for the general tube solutions and by superimposing the relations for the upstream and downstream surfaces (eqs. (21) and (27)). The procedure is illustrated in sketches (m) and (n).

(m)

(n)
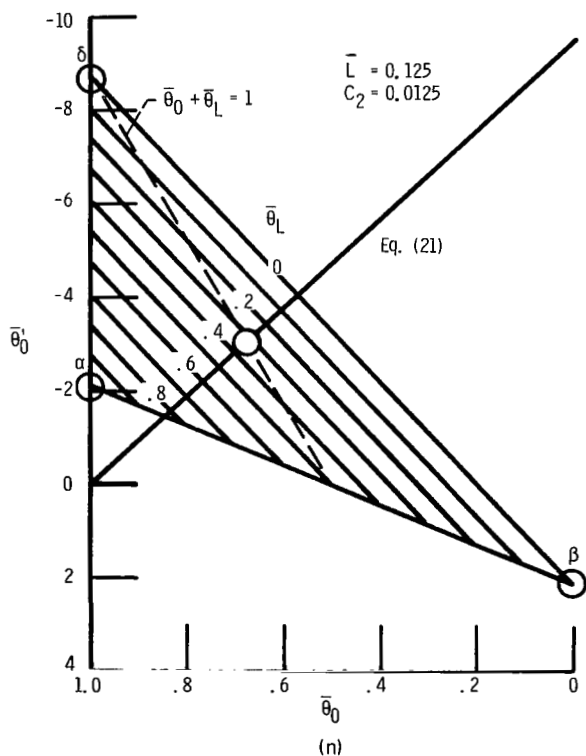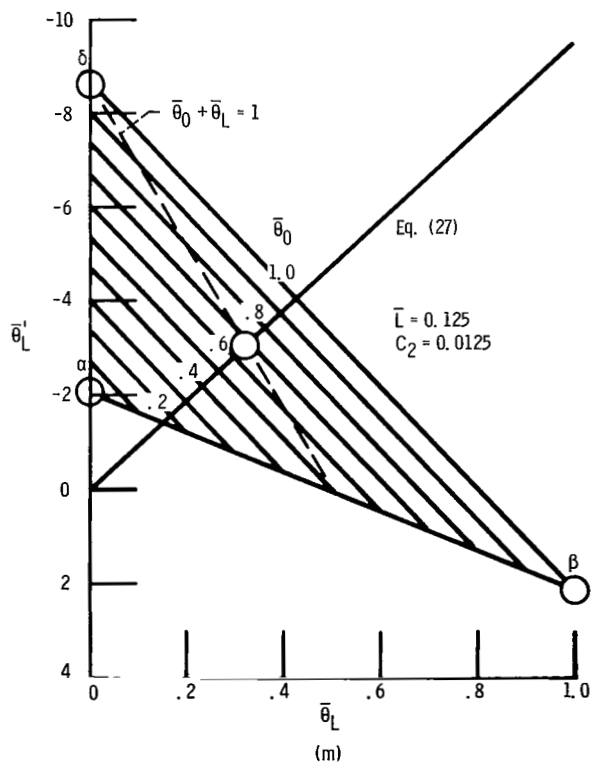
In sketch (m), the ordinate is the slope at the downstream end of the tube, while in sketch (n) it is the upstream value. From the symmetry of the two plots it may be readily shown that the solution must be along the line $\bar{\theta}_O + \bar{\theta}_L = 1.0$, so that actually only one map is required to obtain the solution. For example, (at $\bar{r} = \bar{R}$) equations (21) and (27) and the matching relations (30) may be combined to give the relation

$$\frac{\bar{\theta}'_O}{\bar{\theta}'_L} = \frac{1 - \bar{\theta}_O}{\bar{\theta}_L}$$

The general tube solutions, illustrated by sketches (m) and (n), may also be expressed mathematically as

$$\bar{\theta}'_L = f_1(\bar{\theta}_O) + b_1 \bar{\theta}_L$$

and

$$\bar{\theta}'_O = f_1(1 - \bar{\theta}_L) + b_1(1 - \bar{\theta}_O)$$

where $f_1(\bar{\theta}_O)$ and $f_1(1 - \bar{\theta}_L)$ are the intercepts in (m) and (n), respectively, and b_1 is the slope of the lines. Combining these two expressions gives

$$\frac{\bar{\theta}'_O}{\bar{\theta}'_L} = \frac{f_1(1 - \bar{\theta}_L) + b_1(1 - \bar{\theta}_O)}{f_1(\bar{\theta}_O) + b_1 \bar{\theta}_L}$$

This expression combines with the first relation to give

$$\frac{1 - \bar{\theta}_O}{\bar{\theta}_L} = \frac{f_1(1 - \bar{\theta}_L) + b_1(1 - \bar{\theta}_O)}{f_1(\bar{\theta}_O) + b_1 \bar{\theta}_L}$$

Cross multiplication and simplification of this last expression yield the relation
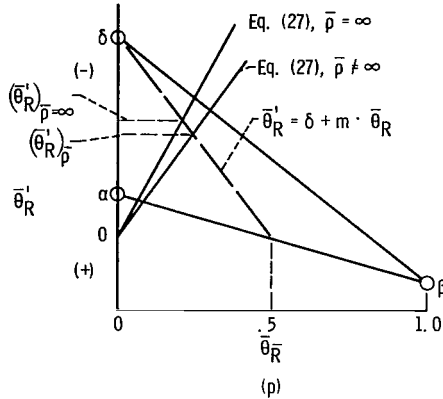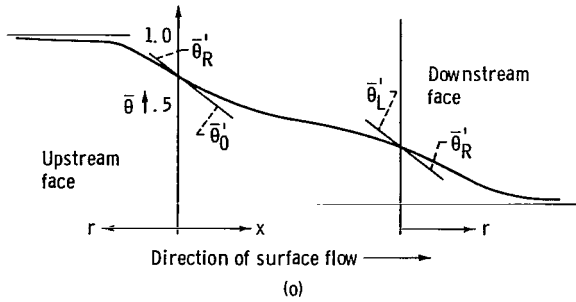
$$(1 - \bar{\theta}_O)f_1(\bar{\theta}_O) = \bar{\theta}_L f_1(1 - \bar{\theta}_L)$$

which further reduces to

$$1 - \bar{\theta}_O = \bar{\theta}_L$$

since $f_1(\bar{\theta}_O)$ equals $f_1(1 - \bar{\theta}_L)$ when $\bar{\theta}_L = 1 - \bar{\theta}_O$. The matched-boundary solutions thus have the properties

$$\bar{\theta}_O + \bar{\theta}_L = 1.0$$

Upstream
face

Downstream
face

1.0

$\bar{\theta}$ ↑ .5

$\bar{\theta}_R'$

$\bar{\theta}_L'$

$\angle\bar{\theta}_0'$

$\bar{\theta}_R'$

r ←——→ x

r ←——→ r

Direction of surface flow ——→

(o)

Eq. (27), $\bar{\rho} = \infty$

Eq. (27), $\bar{\rho} \neq \infty$

$\bar{\theta}_R' = \delta + m \cdot \bar{\theta}_R$

δ

(-)

$(\bar{\theta}_R')_{\bar{\rho}=\infty}$

$(\bar{\theta}_R')_{\bar{\rho}}$

$\bar{\theta}_R'$

α

0

(+)

β

0   .5   1.0

$\bar{\theta}_R$

(p)

$$\bar{\theta}_0' = \bar{\theta}_L'$$

It should be noted that the direction in which the coordinates x and r have been taken herein requires that the matched slopes at the upstream end be equal in magnitude but opposite in sign. This is illustrated in sketch (o) showing a typical complete solution.

The solutions to equation (9), which are matched to the end-face solutions through the boundary conditions of equations (30) and for $\bar{\rho} = \infty$, are presented in table III. A plot of the solutions for $\bar{\theta}_L$ for these matched-flow cases is shown in figure 5, which shows $\bar{\theta}_L$ variations with $\bar{L}$ for various constant values of $C_2/\bar{L}$. The corresponding values of the surface-transmission factor P_S for these same conditions are shown in figure 6. Figure 7 shows the variation in the total transmission factor with tube length for various constant values of $C_2/\bar{L}$. The lower curve of figure 7 represents gas-phase flow only. Clearly, the surface-diffusion flow can become a large fraction of the total flow as C_2 becomes large. The calculations presented herein are also seen to extrapolate very nicely to the long tube limits as calculated from the relations of reference 10.

The matched-boundary-condition solutions for the single tube ($\bar{\rho} = \infty$) may also be examined with regard to their applicability to porous materials having capillarylike pores. As depicted in sketch (o), the slope of the upstream and downstream surface solutions approach zero with increasing r. The solutions would be expected to be valid for pore spacings that allowed this condition to be approached. As was pointed out previously (see the section Upstream and Downstream Surfaces), the appropriate curve of figure 1 may be used to obtain the exact solution applicable to a given pore spacing. The parameter ρ would be equivalent to one-half the distance between pore centers (sketch (a)).

The function $\mathscr{F}(C_2)$, plotted in figure 1, when multiplied by the $\bar{\theta}_R$ yields the slope at $\bar{R}$ (see eq. (27)). The change in this function when $\bar{\rho}$ is less than infinity can thus be used to obtain the change in slope, and hence in surface flow for closely spaced capillaries. The relation is derived as follows with the aid of sketch (p), where the coordinates have been changed from the corresponding maps of sketches (m) and (n) by using the matching relations (30).

The solution $(\bar{\theta}_R')_{\bar{\rho}}$ is obtained by simultaneous solution of the two equations

$$\bar{\theta}_R' = \bar{\theta}_R \, \mathscr{F}(C_2)_{\bar{\rho}} \qquad (44a)$$

and

$$\bar{\theta}_R' = \delta + m\bar{\theta}_R \qquad (44b)$$

Equation (44b) corresponds to the relation $\bar{\theta}_O + \bar{\theta}_L = 1.0$ in terms of the parameters of sketch (p).

The solution for the slope is

$$\left(\bar{\theta}_R'\right)_{\bar{\rho}} = \frac{\mathscr{F}(C_2)_{\bar{\rho}}}{\mathscr{F}(C_2)_{\bar{\rho}} - m} \, \delta \qquad (45)$$

The corresponding solution for $\bar{\rho} = \infty$ is the same as that for equation (45) with $\mathscr{F}(C_2)_{\bar{\rho}=\infty}$ replacing $\mathscr{F}(C_2)_{\bar{\rho}}$. Thus, the ratio of the slope for finite $\bar{\rho}$ to that for $\bar{\rho} = \infty$ is

$$\frac{\left(\bar{\theta}_R'\right)_{\bar{\rho}}}{\left(\bar{\theta}_R'\right)_{\bar{\rho}=\infty}} = \frac{\mathscr{F}(C_2)_{\bar{\rho}}}{\mathscr{F}(C_2)_{\bar{\rho}=\infty}} \; \frac{\mathscr{F}(C_2)_{\bar{\rho}=\infty} - m}{\mathscr{F}(C_2)_{\bar{\rho}} - m} \qquad (46)$$

The values for the slope m are included in table I, and values of the function $\mathscr{F}(C_2)$ are plotted in figure 1. Thus, the solutions for closely spaced pores ($\bar{\rho}$ less than infinity) can be obtained from the single tube solutions (i.e., $\bar{\rho} = \infty$) and equation (46).

As an example, the case of $C_2 = 10$, $\bar{\rho} = 2$, and is presented in the following table:

$\bar{L}$	$\mathscr{F}(10)$ (fig. 1)		m (table I)	$(\bar{\theta}_R')_{\bar{\rho}=2}/(\bar{\theta}_R')_{\bar{\rho}=\infty}$ (Eq. (44))
	$\bar{\rho} = 2$	$\bar{\rho} = \infty$		
1	0.14	0.68	-2.015	0.258

For this illustrative example, then, the slopes and hence the surface transmission probabilities (eq. (39)) for the closely spaced pores ($\bar{\rho} = 2$) would be smaller than that for the corresponding single tube cases by the factors shown.

Comparison of Results with Those of Other Investigators

In reference 1 two systems, silver on molybdenum and silver on nickel, were investigated. The values of the physical parameters cited therein and also used herein, are given in the following table (notation of the present paper being used in all cases):

System	$Q,$ eV	$\tau_0,$ sec	$\mathscr{D},$ cm^2/sec
Silver-molybdenum	2.0	10^{-10}	10^{-4}
Silver-nickel	1.5	10^{-8}	10^{-4}

The resulting values of P_S, the ratio of surface-diffusion flow at the exit to the gas-phase flow at the inlet are compared in the following table:

System	$T,$ $^{\circ}K$	$L,$ cm	$R,$ cm	P_S	
				Ref. 1	Present report
Silver-molybdenum	1000	0.005	0.05	0.27	0.20
Silver-nickel	1000	.005	.05	.15	.086
Silver-nickel	1280	.005	.025	.021	.017
Silver-nickel	1280	.001	.025	.037	.023
Silver-nickel	1280	.005	.10	.005	.0046

It can be seen that the values of P_S of the present paper are all lower than those of reference 1. This is expected since one of the assumptions of reference 1 was that $\theta_0 = \theta_\infty$, which is higher than the value solved for herein, and thus leads to somewhat higher flow by surface diffusion in the tube.

A direct comparison of the results of the present calculations with those of reference 5 is difficult to make because of the differences in the forms of the adsorption isotherms used. The present results are based on a linear adsorption relation (eq. (5)), which, as previously pointed out, is generally acceptable in representing most adsorption relations at low coverage. In reference 5, the evaporation rate data for the cesium-tungsten system (ref. 17) have been used. These data are very nonlinear in the range used therein, as can be seen in sketch (q). This sketch shows the evaporation rate curves for atoms, ions, and for the total of ions plus atoms for a surface temperature of 1400° K. In the absence of an electric field to remove ions from the surface, atoms alone will evaporate. If a sufficiently strong electric field exists at the surface to remove the ion current, both ions and atoms evaporate. Under these conditions, at low coverage the ion component is the major portion of the total evaporation rate. To use a linear relation to
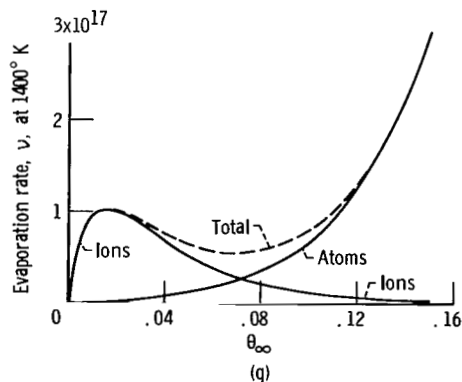
(q)

19

approximate either the atom or ion evaporation rate, obviously means restricting the solutions to cases where θ_∞ is no greater than about 0.08 for the atoms or about 0.01 for the ions.

The use of the total evaporation rate curves as the adsorption isotherm relation in the solution of equation (9), as was done in reference 5, involves the simultaneous assumptions that an electric field exists to remove ions but that the ion trajectories are not then influenced by this field.

Thus neither the approach of reference 5 nor the present one appears adequate to calculate the case for total ion plus atom evaporation of the cesium-tungsten system at coverage fractions above approximately 0.01.

CONCLUDING REMARKS

The object of this report was to analyze the flow characteristics of a cylindrical tube, or pore, under conditions of free-molecule flow with surface diffusion. The integrodifferential equation that describes the flow in the tube was solved numerically for a wide range of variables. Matching boundary conditions were utilized to obtain solutions that included upstream- and downstream-face surface-diffusion flow as well. Transmission factor relations were developed that allow quantitative comparisons to be made of the differences between flow with and without surface-diffusion effects.

In general, it was found that with the inlet and exit surface coverage fractions held fixed, the shape of the curves describing the surface coverage fraction in the tubes varied as follows: with a large value of the surface-diffusion flow parameter, solutions were nearly straight lines between end points; as the parameter decreased, the curves approached the nearly straight-line solutions of zero surface-diffusion flow except for the fixed end points.

Matched-boundary-condition solutions were found to be obtainable from maps of general solutions for a given tube length and surface-diffusion flow parameter for either a single tube or for a closely spaced array of tubes. The matched solutions were presented only for the single tube model, but relations were derived that permit the application of these results to porous media models made up of closely spaced capillaries. Transmission factors were found to increase with increased surface-diffusion flow parameter, the increase being proportionally much greater with longer tubes.

Comparison of results with one investigator showed excellent agreement. In another comparison, differences were attributable to dissimilar basic assumptions or boundary conditions for the model.

Lewis Research Center,
    National Aeronautics and Space Administration,
        Cleveland, Ohio, October 21, 1965.

20

SYMBOLS

[Unless otherwise specified, cgs units are used throughout.]

A	parameter defined in eq. (B1)
a	distance between adsorption sites
B	parameter defined in eq. (B1)
b	parameter defined in eq. (15)
b_1	slope of lines of general solution maps (sketches (l) and (m))
C_1	parameter defined in eqs. (C1) to (C5)
C_2	parameter defined in eq. (11)
C_3	parameter defined in eq. (14)
c	parameter defined in eq. (15)
$\mathscr{D}$	surface-diffusion coefficient, cm^2/sec
$F_{1,2}$	geometric factor defined in eq. (2)
$F_{3,2}$	geometric factor defined in eq. (3)
$\mathscr{F}(C_2)$	function defined by eq. (29)
f	parameter defined in eq. (C3)
f_1	function giving intercept of lines in sketches (m) and (n)
g	parameter defined in eq. (C5)
I_0	modified Bessel function of the first kind of order zero
I_1	modified Bessel function of the first kind of first order
K_0	modified Bessel function of the second kind of order zero
K_1	modified Bessel function of the second kind of first order
k	Boltzmann constant, $erg/^\circ K$
L	tube length, cm
M	mass of atom or molecule, g

m	slope of lines on general solution maps for which $\bar{\theta}_O + \bar{\theta}_L = 1.0$ (see table I and sketch (p))
n_1	gas-phase flow rate into tube, atoms/sec
n_2	surface-diffusion flow rate into tube, atoms/sec
n_3	gas-phase flow rate out of tube, atoms/sec
n_4	surface-diffusion flow rate out of tube, atoms/sec
P_d	direct transmission factor, fraction of entering gas-phase flow particles that exit downstream without experiencing any collisions with tube wall
P_G	sum of P_i and P_d
P_i	indirect transmission factor, fraction of entering gas-phase flow particles that exit downstream after experiencing one or more collisions with tube walls
P_S	ratio of surface-diffusion flow at exit to entering gas-phase flow
P_T	total transmission factor
p	pressure, dyne/cm^2
Q	desorption energy, eV
R	tube radius, cm
r	radial distance variable
T	temperature, ^{O}K
T_{eV}	temperature expressed in electron volts, $T_{eV} = \dfrac{T}{11\ 605}$
t	time, sec
v	velocity, cm/sec
x	axial distance variable, cm
x_2	axial distance variable at specific location (see sketch (b)), cm
α, β, δ	designation of general solution points (see table I)
γ	sticking coefficient
ϵ	convergence criterion defined in eq. (38)

θ fraction of monolayer surface coverage

θ' gradient in fractional surface coverage with respect to nondimensional distance variable

θ'' second derivative of θ with respect to nondimensional distance variable

θ_0 value of surface coverage fraction in tube at inlet

θ_0' gradient of surface coverage fraction in tube at inlet

θ_L value of surface coverage fraction in tube at exit

θ_L' gradient of surface coverage in tube at exit

θ_R surface coverage fraction on upstream or downstream face at tube radius R

θ_R' gradient in surface coverage fraction on either face at tube radius R

θ_∞ maximum surface coverage fraction attainable in system

μ arrival rate, atoms/(cm^2)(sec)

μ_1 arrival rate at conditions existing in inlet chamber, atoms/(cm^2)(sec)

ν rate of particles leaving surface, atoms/(cm^2)(sec)

ν_d particle leaving rate from downstream face, atoms/(cm^2)(sec)

ρ radial distance at which concentration gradient becomes zero

σ surface concentration, atoms/cm^2

σ' surface concentration gradient with respect to nondimensional distance variable, atoms/cm^2

σ'' second derivative of σ with respect to nondimensional distance variable, atoms/cm^2

σ_m surface concentration for a filled monolayer, atoms/cm^2

τ adsorption time, sec

τ_m time to form monolayer (defined in eq. (6)), sec

τ_0 constant in eq. (C7), equal to 10^{-13} sec in typical calculations

Superscript:

$^-$ Barred distance quantities refer to nondimensional ratios of the variable to the tube radius R (e.g., $\bar{L} = L/R$); barred parameters involving θ refer to ratios of the variable to the value θ_∞ (e.g., $\bar{\theta}_0 = \theta_0/\theta_\infty$)

APPENDIX B

APPROXIMATION OF EQUATION (1)

As mentioned in the report, the solution of equation (1) is nearly linear. As a result, it has been approximated by a relation of the following form:

$$\frac{\nu(\overline{x})}{\mu_1} \cong A + B\overline{x} \tag{B1}$$

The true solution also has the property

$$\frac{\nu(\overline{x})}{\mu_1} + \frac{\nu(\overline{L} - \overline{x})}{\mu_1} = 1 \tag{B2}$$

as has been shown to be required based on thermodynamic arguments (refs. 8 and 11). Using equation (B2), the quantity B can be expressed in terms of A.

$$B = \frac{1 - 2A}{\overline{L}} \tag{B3}$$

Substituting into equation (B1) yields

$$\frac{\nu(\overline{x})}{\mu_1} \cong A\left(1 - 2\,\frac{\overline{x}}{\overline{L}}\right) + \frac{\overline{x}}{\overline{L}} \tag{B4}$$

The parameter A (the value of $\nu(0)/\mu_1$) can be determined approximately by assuming equation (B4) to be a solution to equation (1), substituting, performing the integration, and evaluating the resultant expression at $\overline{x} = 0$, or $\overline{x} = \overline{L}$. The result is

$$A \cong \frac{1 + \dfrac{\overline{L}}{2} - \dfrac{\overline{L}^2}{2\sqrt{\overline{L}^2 + 4}}}{1 + \dfrac{2}{\sqrt{\overline{L}^2 + 4}}} \tag{B5}$$

This result was also noted in references 6 and 19; however, the expression in reference 19 differs from equation (B5). The reason for the difference is not known. It may be due to a translation error.

The agreement between the A values obtained from equation (B5) and the end-point values obtained from converged numerical solutions (ref. 8) is within 1 percent as shown in the following table:

24

$\overline{L}$	$\nu(0)/\mu_1$ (ref. 8)	A (eq. (B5))
0.5	0.6037	0.6074
1.0	.6738	.6736
2.0	.7576	.7574
4.0	.8366	.8369
8.0	.8990	.9010
16.0	.9417	.9450

The variation of A with $\overline{L}$ is plotted in figure 8. The values can be used with equation (B4), when no greater accuracy is required, to obtain values of wall fluxes in the absence of surface-diffusion effects. More accurate values for cylindrical tubes as well as for convergent and divergent tubes are available in reference 8.

APPENDIX C

ADSORPTION ISOTHERMS

The discussion of adsorption isotherm relations included herein is intended merely to give an insight into the subject. Detailed discussions may be found in references 22 and 23. The type of relation utilized for a given system is usually governed by the assumptions made with respect to the following factors:

(a) Adsorbed film mobility: The classification of an adsorbed film as mobile or immobile depends on the relative values of the energy barriers to diffusion and to evaporation. If the energy barrier to surface diffusion is low compared with the evaporation energy, the particles will migrate for some time before they are apt to leave the surface; hence the film is classed as mobile.

(b) Variation of adsorption energy (binding energy) with surface concentration: Adsorption energy may vary because of surface inhomogeneities. It may also vary because of dipole interactions among the adsorbed species.

(c) Relative surface concentration: Certain forms of the adsorption isotherm relation have a filled monolayer as the limiting concentration; others do not restrict adsorption to a monolayer but permit multilayer adsorption. This distinction also generally depends upon the relative adsorption energies of the gas for the substrate and of the gas for itself.

A summary of some of the various forms for the adsorption isotherm relation from reference 23 is as follows:

Mobile film (no interaction)

$$\mu = C_1 \theta \tag{C1}$$

and

$$\mu = C_1 \frac{\theta}{1 - \theta} \exp\left(\frac{\theta}{1 - \theta}\right) \tag{C2}$$

Mobile film (interaction)

$$\mu = C_1 \frac{\theta}{1 - \theta} \exp\left(\frac{\theta}{1 - \theta} - f\theta\right) \tag{C3}$$

Immobile film (no interaction)

$$\mu = C_1 \frac{\theta}{1 - \theta} \tag{C4}$$

Immobile film (interaction)

$$\mu = C_1 \frac{\theta}{1 - \theta} \exp(-g\theta) \tag{C5}$$

where μ is the arrival rate, C_1 is a proportionality constant, and θ is the surface concentration expressed as a fraction of a monolayer.

Equations (C1) and (C4) are the simplest of the preceding relations. Equation (C1) is not bounded and permits coverages in excess of a monolayer. Equation (C4), usually referred to as the Langmuir adsorption relation (ref. 23), represents the behavior characteristic of many systems of interest where the adsorption energy of the gas for the substrate is considerably greater than the adsorption energy of the gas for itself (i.e., the sublimation energy). In this case, adsorption is usually restricted to less than a monolayer until gas-phase arrival rates (or corresponding gas pressures) approach the saturation value corresponding to the temperature of the adsorbing surface.

Equation (C4) can be derived from a simple dynamic equilibrium approach. The evaporation rate is assumed to vary directly with the surface concentration σ of adsorbed particles and inversely with the average adsorption time τ (ref. 22):

$$\nu = \frac{\sigma}{\tau} = \frac{\sigma_m \theta}{\tau} \tag{C6}$$

The adsorption time τ is related to the desorption energy Q:

$$\tau = \tau_0 \exp\left(\frac{Q}{T_{eV}}\right) \tag{C7}$$

The adsorption rate is assumed equal to the product of the arrival rate μ, the sticking coefficient γ, and the area available for adsorption $1 - \theta$. In equilibrium the adsorption rate equals the vaporization rate so that

$$\nu = \mu\gamma(1 - \theta) = \theta \frac{\sigma_m}{\tau_0} \exp\left(- \frac{Q}{T_{eV}}\right) \tag{C8}$$

or

$$\mu = C_1 \frac{\theta}{1 - \theta} \tag{C9}$$

where

$$C_1 = \frac{\sigma_m}{\gamma\tau_0} \exp\left(- \frac{Q}{T_{eV}}\right) \tag{C10}$$

27

From equation (C8) it can be seen that for $\gamma = 1$ and low values of θ

$$\nu = \mu \cong C_1\theta \qquad (C11)$$

This is identical with equation (5), and, in fact, all the adsorption isotherm relations approach this form for low θ. As a result, the solutions of the flow relations obtained in this report are based on a relation of the form of equation (C11). They can be considered characteristic of systems having constant adsorption energy over the range of surface concentration considered and for which the isotherm behavior described by equation (C1) applies without limit to θ. For the other isotherm relations they are restricted to systems with low θ values.

NUMERICAL SOLUTION OF EQUATION (9)

by Carl D. Bogart
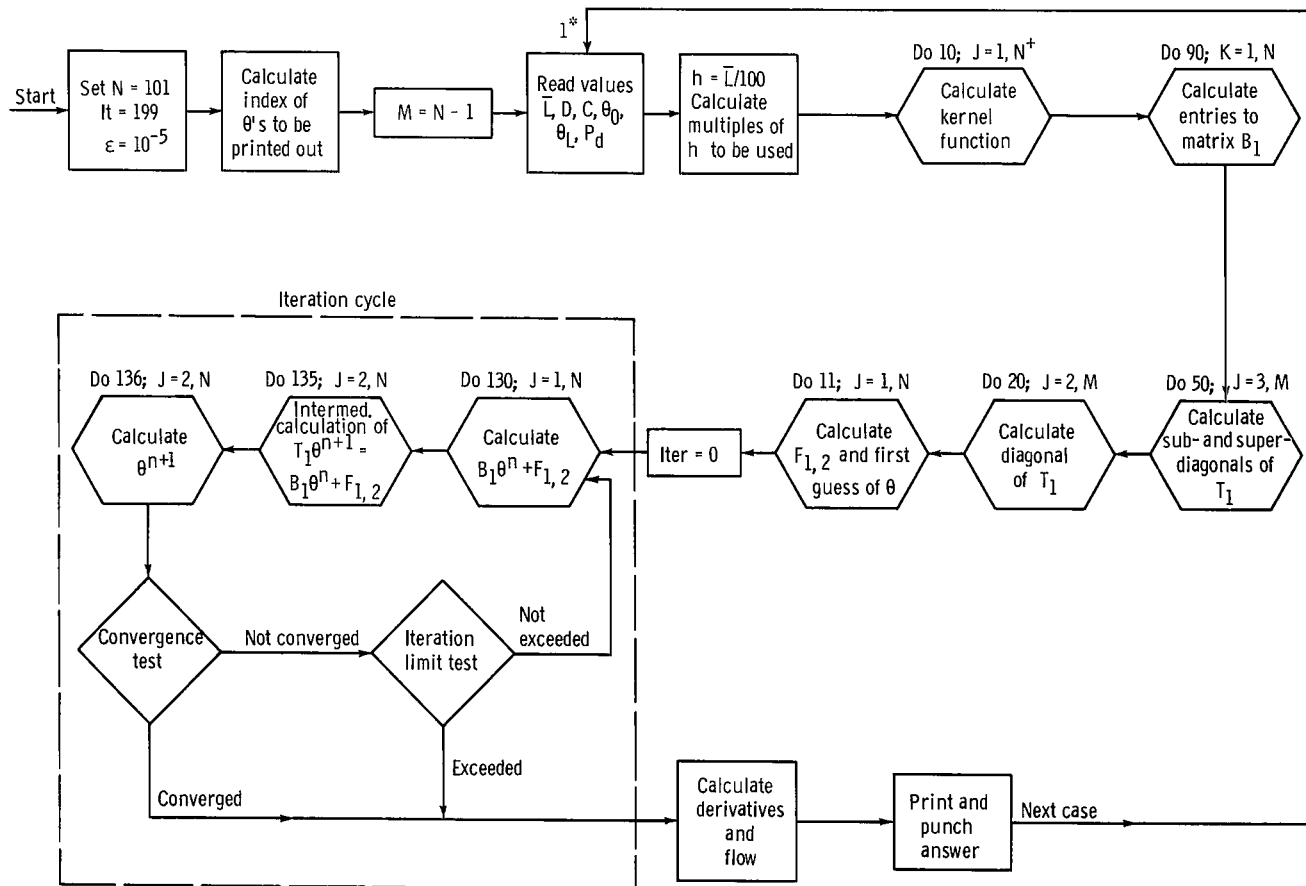
Equation (9) can be written in finite difference form as

$$\theta(x_i) = F_{1,2}(x_i) + \frac{2h}{3}\left[F_{3,2}(x_i,0)\theta_0 + 4F_{3,2}(x_i,h)\theta_1 + \right.$$

$$\left. 2F_{3,2}(x_i,2h)\theta_2 + \ldots\right] + \frac{C_2}{h^2}\left[\theta(x_{i+1}) + \theta(x_{i-1}) - 2\theta(x_i)\right]$$

where the integral has been expanded by Simpson's rule and the second derivative by a three point formula. The notation is as follows: $x_i = ih$, where $i = 0, 1, \ldots, N - 1$; $h = L/(N - 1)$; and $F_{3,2}(x_i,ih)$ is the kernel function of the integral with $\theta(x_i) \equiv \theta_i$. This arrangement results in N linear equations in N unknowns, which can be written in matrix form as $A_1\theta = F_{1,2}$. Since the values of θ at $x = 0$ and $x = L$ are specified, the integro-differential equation has a unique solution.

By inspection, the matrix A_1 is tridiagonally dominant because the terms on the diagonal, subdiagonal and superdiagonal are on the order of C^2/h^2. The mesh increment h may be chosen small enough so that $C^2/h^2 \geq 10^2$ and the absolute value of any other terms is less than unity. By the theory of regular splittings (ref. 24), the matrix equation may be written as $(T_1 - B_1)\theta = F_{1,2}$, where T_1 is a matrix having only the tridiagonal terms and B_1 has no tridiagonal entries. The iterative scheme then becomes $T_1\theta^{n+1} = B_1\theta^n + F_{1,2}$, where n denotes the nth iterate ($n = 0, 1, 2, \ldots$). An initial guess is supplied for θ and rapid convergence results since $B_1\theta^n$ represents only a small correction and θ^{n+1} may be calculated explicity by an algorithm for solving tridiagonal systems (ref. 24).

A schematic flow chart and Fortran IV listing of the computer program are as follows:

Flow chart

Start →
Set N = 101
It = 199
$\epsilon = 10^{-5}$
→ Calculate index of θ's to be printed out → M = N - 1 → 1^* Read values $\bar{L}, D, C, \theta_0, \theta_L, P_d$ → h = $\bar{L}/100$ Calculate multiples of h to be used → Do 10; J = 1, N^+ Calculate kernel function → Do 90; K = 1, N Calculate entries to matrix B_1

Do 50; J = 3, M Calculate sub- and super-diagonals of T_1 → Do 20; J = 2, M Calculate diagonal of T_1 → Do 11; J = 1, N Calculate $F_{1,2}$ and first guess of θ → Iter = 0 → Do 130; J = 1, N Calculate $B_1\theta^n + F_{1,2}$ → Do 135; J = 2, N Intermed. calculation of $T_1\theta^{n+1} = B_1\theta^n + F_{1,2}$ → Do 136; J = 2, N Calculate θ^{n+1}

Iteration cycle

Convergence test → Not converged → Iteration limit test → Not exceeded

Converged / Exceeded → Calculate derivatives and flow → Print and punch answer → Next case

*Fortran statement numbers

$^+$Fortran do statement

```
$IBFTC REYNO    DEBUG,LIST,NODECK,REF
        DIMENSION G(101),KER(101),AA(101,101),F(101),Y(101),A1(101)
        DIMENSION WW(101),GG(101),A2(101),A3(101)
        DOUBLE PRECISION AA,A1,A2,  AB,     AC,     A,     C,    DH2,
     2          DH,     D,     ED,    EPS,     F.     G,     H6,     H,
     3          KER,   LBAR,   SUM,    XJ,     Y              ,EP
        DOUBLE PRECISION GG,WW,SAV,A3
        DIMENSION INDEX(27)
        DATA N/101/
        DATA IT,EP/199,1.D-5/
C LBAR=L
C H=MESH SIZE
C D=MULTIPLIER OF D2THETA/DX2
C D IS ACTUALLY D/C
C LBAR/H MUST BE EVEN
C LBAR/H MUST BE LESS THAN OR EQUAL TO 100
C C IS MULTIPLIER OF Y-FUNCTION
        WRITE(6,100)
  100   FORMAT(1H1)
C    INDEX OF VALUES TO BE PRINTED
        DO 162 J=1,6
        L=2*(J-1)
        INDEX(J)=L
  162   INDEX(J+21)=L+90
        DO 163 J=7,21
        L=5*(J-4)
  163   INDEX(J)=L
        M=N-1
    1   READ(5,105) RLBAR,RD,RC,READ1,READ2,PD
        LBAR=RLBAR
        D=RD
        C=RC
        H=.01D0*LBAR
        H3=H/3.
        H6=H/6.D0
        DO 10 J=1,N
        XJ=J-1
        XJ=XJ*H
        AB=XJ**2+4.D0
        AC=DSQRT(AB)
   10   KER(J)=1.D0-XJ*(XJ**2+6.D0)/(AB*AC).
C    SET UP FINITE DIFF EQNS
        DO 90 K=1,N
        JJ=N-K+1
        AA(K,N)=-H6*KER(JJ)
        AA(K,1)=-H6*KER(K)
        AA(K,K)=0.D0
        L=K-1
        LL=K+1
        IF(K.GT.1) AA(K,L)=0.D0
        IF(K.LT.N) AA(K,L)=0.D0
        L=L-1
        LL=LL+1
        IF(L.LT.2) GO TO 60
        DO 70 J=2,L
        XJ=4-2*MOD(J,2)
        I=K-J+1
   70   AA(K,J)=-XJ*H6*KER(I)
   60   IF(LL.GT.M) GO TO 90
        DO 30 J=LL,M
```

31

```
           XJ=4-2*MOD(J,2)
           I=J-K+1
   30      AA(K,J)=-XJ*H6*KER(I)

   90      CONTINUE
           DH=D/H**2
           DH2=2.D0*DH+1.D0
           DO 50 J=3,M
           XJ=4-2*MOD(J,2)
           A3(J-1)   =-DH-XJ*H6*KER(2)
           XJ=4-2*MOD(J-1,2)
   50      A2(J  )   =-DH-XJ*H6*KER(2)
           DO 20 J=2,M
           XJ=4-2*MOD(J,2)
   20      A1(J)=DH2-XJ*H6
           A2(2)   =-DH-H6*KER(2)
           A3(N-1)=A2(2)
           DO 11 J=1,N
           XJ=J-1
           XJ=XJ*H
           AB=XJ**2+4.D0
           AC=DSQRT(AB)
           G(J)=.5D0*((XJ**2+2.D0 )/AC-XJ)/C
   11      F(J)=(LBAR+1.D0-XJ)/(C*(LBAR+2.D0))
C    MATRIX ENTRIES TO ALLOW END VALUES TO REMAIN FIXED
           A2(N)=0.D0
           A3(1)=0.D0
           A1(N)=1.D0
           A1(1)=1.D0
           A3(N)=0.D0
           A2(1)=0.D0
           DO 99 J=1,N
           AA(1,J)=0.
   99      AA(N,J)=0.
C    READ1 IS VALUE OF FUNCTION AT X=0
           F(1)=READ1
           G(1)=F(1)
C    READ2 IS VALUE OF FUNCTION AT X=L
           F(N)=READ2
           G(N)=F(N)
           ITER=0
C   BEGIN ITERATION CYCLE
  115      DO 130 J=1,N
           SUM=G(J)
           DO 133 JJ=1,N
  133      SUM=SUM-AA(J,JJ)*F(JJ)
  130      Y(J)=SUM
           WW(1)=A3(1)/A1(1)
           GG(1)=Y(1)/A1(1)
           DO 135 J=2,N
          GG(J)=(Y(J)-A2(J)*GG(J-1))/(A1(J)-A2(J)*WW(J-1))
  135      WW(J)=A3(J)/(A1(J)-A2(J)*WW(J-1))
           NNL=N
           SAV=F(N)
           F(N)=GG(N)
           EPS=DABS((SAV-F(N))/F(N))
           K=N-1
           DO 136 J=2,N
           SAV=F(K)
           F(K)=GG(K)-WW(K)*F(K+1)
           A=DABS((SAV-F(K))/F(K))
```

```fortran
          IF(A.LE.EPS) GO TO 136
          EPS=A
          NNL=K
  136     K=K-1
          ITER=ITER+1
C    CONVERGENCE TEST
          IF(EPS.LE.EP) GO TO 160
  151     IF(ITER.LE.IT )GO TO 115
  160     Y(101)=0.
          RB=0.
          DO 170 J=1,21
          RA=RB**2
          RC=1.-RA
          RD=1.+RA
          FRA=-4.*RA
          DO 180 L=1,100
          XL=L-1
          XL=LBAR-XL*H
          XR=XL**2
          Y(L)=F(L)*XL*(XR+RC)/((XR+RD)**2+FRA)**1.5
  180     CONTINUE
          S1=0.
          S2=0.
          DO 181 L=2,N,2
          S1=S1+Y(L)
  181     S2=S2+Y(L+1)
          WW(J)=H3*(Y-Y(101)+4.*S1+2.*S2)*RB
  170     RB=RB+.05
          S1=0.
          S2=0.
          DO 182 J=2,20,2
          S1=S1+WW(J)
  182     S2=S2+WW(J+1)
          PIND=.2*C*(WW-WW(21)+4.*S1+2.*S2)/3.
          DTH1=(F(2)-F)/H
          DTHL=(F(N)-F(N-1))/H
          PG=PIND+PD
          DO 164 J=1,27
          L=INDEX(J)+1
  164     Y(J)=F(L)
          PS=2.*D*C*DTHL
C    PRINT ANSWERS
          WRITE(6,101) LBAR,D,C,READ1,READ2,DTH1,DTHL
          WRITE(6,102) ITER,EPS,PIND,PG,PS,H
          WRITE(6,103)(INDEX(J),Y(J),J=1,27)
          Y(28)=DTH1
          Y(29)=DTHL
          Y(30)=ITER
          Y(31)=EPS
          Y(32)=PIND
          CALL BCDUMP(Y(1),Y(32))
          WRITE(6,104)
          WRITE(6,104)
          GO TO 1
  101     FORMAT(6H LBAR=F7.4,3H,D=F15.8,3H,C=F2.0,9H,THETA 0=G15.8,
     *    9H,THETA L=G15.8,8H,DTHDX0=G15.8,8H,DTHDXL=G15.8)
  102     FORMAT(6H ITER=I3,5H,EPS=F8.6,6H,PIND=G14.8,4H,PG=G14.8,
     *    4H,PS=G15.8,3H,H=F8.6)
  103     FORMAT(1H09(I4,1PE10.3)/1H 9(I4,1PE10.3)/1H 9(I4,1PE10.3))
  104     FORMAT(1HK)
  105     FORMAT(6F10.5)
          END
```

REFERENCES

1. Winterbottom, W. L.; and Hirth, J. P.: Diffusional Contribution to the
   Total Flow from a Knudsen Cell. J. Chem. Phys., vol. 37, no. 4,
   Aug. 15, 1962, pp. 784-793.

2. Carman, Philip Crosbie: Flow of Gases Through Porous Media. Academic
   Press, Inc., 1956.

3. Dykman, I. M. (M. Nadler, trans.): On the Mechanism of Activator Vapour
   Supply to the Outer Surface of a Porous Metal-Film Cathode. Radio Eng.
   and Electronics Phys., vol. 2, no. 12, 1957, pp. 83-89.

4. Reynolds, Thaine W.; and Kreps, Lawrence W.: Gas Flow, Emittance, and Ion
   Current Capabilities of Porous Tungsten. NASA TN D-871, 1961.

5. Forrester, A. T.; and Bates, T. R.: Cesium Transport Through a Tungsten
   Capillary - An Integral Treatment. Rept. No. RR-24, Electro-Optical
   Systems, Inc., Feb. 1965.

6. Clausing, P.: The Flow of Very Dilute Gases Through Tubes of Any Length.
   Ann. Phys., vol. 12, no. 8, Mar. 10, 1932, pp. 961-989.

7. Patterson, G. N.: A State-of-the-Art Survey of Some Aspects of the
   Mechanics of Rarefied Gases and Plasmas. Rept. No. ARL 64-60, Toronto
   Univ., Apr. 1964.

8. Richley, Edward A.; and Reynolds, Thaine W. (With appendix C by Carl D.
   Bogart): Numerical Solutions of Free-Molecule Flow in Converging and
   Diverging Tubes and Slots. NASA TN D-2330, 1964.

9. Hill, Terrell L.: Surface Diffusion and Thermal Transpiration in Fine
   Tubes and Pores. J. Chem. Phys., vol. 25, no. 4, Oct. 1956, pp. 730-735.

10. Sears, G. W.: A Note on the Flow of Gases Through Very Fine Tubes. J.
    Chem. Phys., vol. 22, no. 7, July 1954, pp. 1252-1253.

11. Sparrow, E. M.; Jonsson, V. K.; and Lundgren, T. S.: Free-Molecule Tube
    Flow and Adiabatic Wall Temperatures. J. Heat Transfer, Trans. ASME,
    ser. C, vol. 85, no. 2, May 1963, pp. 111-118.

12. DeMarcus, W. C.: The Problem of Knudsen Flow. Pt. 1. General Theory.
    Rept. No. K-1302, AEC, Sept. 5, 1956.

13. DeMarcus, W. C.: The Problem of Knudsen Flow. Pt. II. Solution of
    Integral Equations with Probability Kernels. Rept. No. K-1302, AEC,
    Oct. 4, 1956.

14. DeMarcus, W. C.: The Problem of Knudsen Flow. Pt. III. Solutions for
    One-Dimensional Systems. Rept. No. K-1302, AEC, Mar. 19, 1957.

15. DeMarcus, W. C.: The Problem of Knudsen Flow. Pt. IV. Specular Reflection. Rept. No. K-1302, AEC, Mar. 27, 1957.

16. DeMarcus, W. C.: The Problem of Knudsen Flow. Pt. V. Application of the Theory of Radiative Transfer. Rept. No. K-1302, AEC, July 30, 1957.

17. DeMarcus, W. C.; and Jenkins, H. B., Jr.: The Problem of Knudsen Flow. Pt. VI. Tortuosity. Rept. No. K-1302, AEC, Sept. 30, 1957.

18. Levenson, L. L.; Milleron, N.; et Davis, D. H.: Conductance en écoulement moléculaire. (Molecular Flow Conductance.) Le Vide, vol. 18, no. 103, Jan. - Feb. 1963, pp. 42-54.

19. Ivanov, B. S.; and Troitskii, V. S.: Formation of Directivity Patterns of Molecular Beams. Soviet Phys.-Tech. Phys., vol. 8, no. 4, Oct. 1963, pp. 365-368.

20. Honig, R. E.: Vapor Pressure Data for the Solid and Liquid Elements. RCA Rev., vol. 23, no. 4, Dec. 1962, pp. 567-586.

21. Taylor, John Bradshaw; and Langmuir, Irving: The Evaporation of Atoms, Ions and Electrons from Cesium Films on Tungsten. Phys. Rev., vol. 44, no. 6, Sept. 15, 1933, pp. 423-458.

22. DeBoer, J. H.: Adsorption Phenomena. Vol. VIII of Advances in Catalysis, W. G. Frankenburg, V. I. Komarewsky and E. K. Rideal, eds., Academic Press, Inc., 1956, pp. 17-161.

23. Ross, Sydney; and Olivier, James P.: On Physical Adsorption. Intersci. Publ. 1964.

24. Varga, Richard S.: Matrix Iterative Analysis. Automatic Computation Ser., Prentice Hall, Inc., 1962.

TABLE I. - END-POINT SLOPES

Nondimensional tube length, $\overline{L}$	Diffusion parameter, $C_2/\overline{L}$	General solution points			Slope of lines on general solution maps, m
		α	β	δ	
		$\overline{\theta}'_0$ for $\begin{cases}\overline{\theta}_0 - 1.0 \\ \theta_L = 1.0\end{cases}$	$\overline{\theta}'_0$ for $\begin{cases}\overline{\theta}_0 = 0 \\ \theta_L = 0\end{cases}$	$\overline{\theta}'_0$ for $\begin{cases}\overline{\theta}_0 = 1.0 \\ \theta_L = 0\end{cases}$	
		$\overline{\theta}'_L$ for $\begin{cases}\overline{\theta}_0 = 0 \\ \theta_L = 0\end{cases}$	$\overline{\theta}'_L$ for $\begin{cases}\overline{\theta}_0 = 1.0 \\ \theta_0 = 1.0\end{cases}$	$\overline{\theta}'_L$ for $\begin{cases}\overline{\theta}_0 = 1.0 \\ \theta_L = 0\end{cases}$	
1/16	10	-0.02373	0.02422	-16.0062	-32.013
	1	-.2362	.2411	-16.0767	-32.158
	.1	-2.2591	2.308	-16.773	-33.595
	.01	-16.1411	16.588	-23.10	-46.64
1/8	10	-0.02275	0.02371	-8.007	-16.015
	1	-.2254	.2350	-8.0747	-16.159
	.1	-2.072	2.167	-8.743	-17.581
	.01	-12.258	13.061	-14.335	-29.473
1	10	-0.01257	0.0178	-1.0048	-2.0148
	1	-.1196	.1715	-1.048	-2.148
	.1	-.8301	1.2887	-1.427	-3.313
	.01	-3.0089	5.551	-3.374	-9.290
4	10	-0.00269	0.008786	-0.2515	-0.509
	1	-.02522	.08456	-.2644	-.588
	.1	-.1690	.6509	-.3670	-1.216
	.01	-.6609	3.0113	-.8195	-3.989
16	10	-0.000155	0.002526	-0.06261	-0.1276
	1	-.00152	.02488	-.06365	-.1507
	.1	-.0131	.2190	-.07293	-.3517
	.01	-.0708	1.223	-.1228	-1.398

TABLE II. - INDIRECT TRANSMISSION FACTORS

Nondimensional tube length, $\bar{L}$	Diffusion parameter, $C_2/\bar{L}$	Ratio of inlet to maximum surface coverage fraction, $\bar{\theta}_0$		
		1	1	0
		Ratio of exit to maximum surface coverage fraction, $\bar{\theta}_L$		
		1	0	0
1/16	10	0.0436	0.0263	0
	1	.0435	.0263	.00012
	.1	.0425	.0263	.00111
	.01	.0363	.0259	.00732
1/8	10	0.1006	0.0558	0.00006
	1	.1002	.0558	.00053
	.1	.0959	.0557	.00475
	.01	.0764	.0552	.0244
1	10	0.5998	0.2546	0.0015
	1	.5867	.2550	.0141
	.1	.5059	.2589	.0907
	.01	.3739	.2717	.2085
4	10	0.9247	0.2178	0.0019
	1	.9010	.2200	.0169
	.1	.7624	.2345	.0965
	.01	.5192	.2664	.2089
16	10	0.9417	0.0757	0.003
	1	.931	.0767	.0027
	.1	.844	.0842	.0203
	.01	.565	.1065	.0694

<div align="center">TABLE III. — MATCHED BOUNDARY CONDITION SOLUTIONS</div>

$$[\widetilde{\rho} = \infty]$$

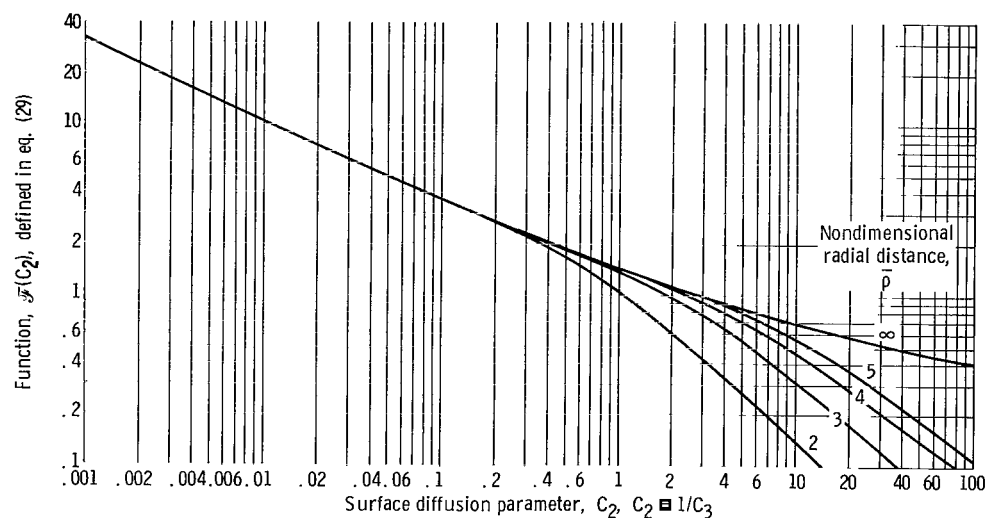| Nondimensional tube length, $\overline{L}$	Diffusion parameter, $C_2/\overline{L}$	Ratio of inlet to maximum surface coverage fraction, $\overline{\theta}_0$	Ratio of exit to maximum surface coverage fraction, $\overline{\theta}_L$	Exit coverage fraction gradient, $\overline{\theta}'_L$	Indirect transmission factor, P_i	Surface transmission factor, P_S	Direct transmission factor, P_d	Total transmission factor, P_T
1/16	10	0.525	0.475	-0.807	0.0220	1.01	0.939	1.971
	1	.562	.438	-1.95	.0224	.244		1.205
	.1	.640	.360	-4.71	.0230	.0589	↓	1.021
	.01	.733	.267	-10.68	.0236	.01335	↓	.976
1/8	10	0.539	0.461	-0.608	0.0507	1.52	0.883	2.454
	1	.585	.415	-1.38	.0513	.345		1.279
	.1	.677	.323	-3.07	.0522	.0768	↓	1.012
	.01	.752	.248	-7.07	.0528	.0177	↓	.954
1	10	0.627	0.373	-0.254	0.289	5.08	0.382	5.751
	1	.707	.293	-.419	.282	.838		1.502
	.1	.798	.202	-.737	.275	.147	↓	.804
	.01	.830	.170	-1.79	.278	.0358	↓	.696
4	10	0.748	0.252	-0.1236	0.342	9.888	0.056	10.286
	1	.820	.180	-.158	.306	1.264		1.626
	.1	.889	.111	-.231	.278	.185	↓	.519
	.01	.915	.0853	-.478	.283	.0383	↓	.377
16	10	0.874	0.126	-0.0465	0.175	14.88	0.004	15.059
	1	.915	.085	-.0508	.143	1.62		1.767
	.1	.953	.047	-.0562	.117	.18	↓	.301
	.01	.972	.028	-.0836	.118	.0267	↓	.149

Figure 1. - Parameters useful for solution of upstream and downstream wall expressions (eqs. (21) and (27)).
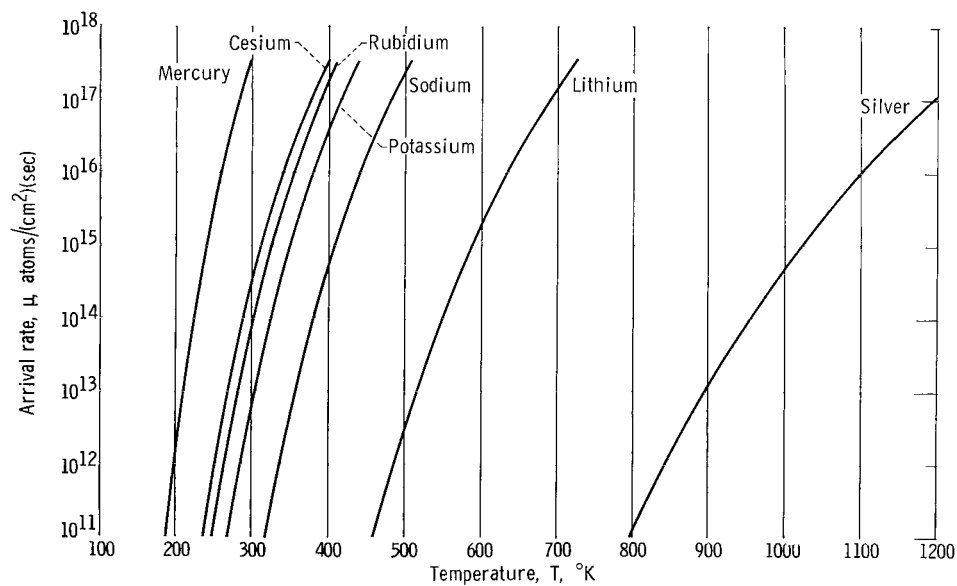

Figure 2. - Variation of equilibrium arrival rate with temperature for various metal vapors (ref. 20 and eq. (41)).
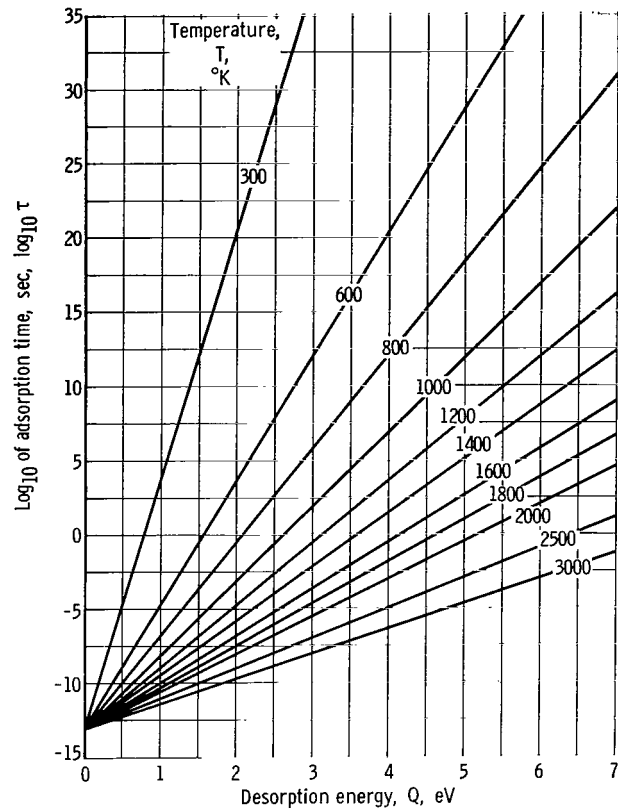
Figure 3. - Variation of adsorption time with energy for various temperatures. Constant, $\tau_0 = 10^{-13}$ second (eq. (C7)).
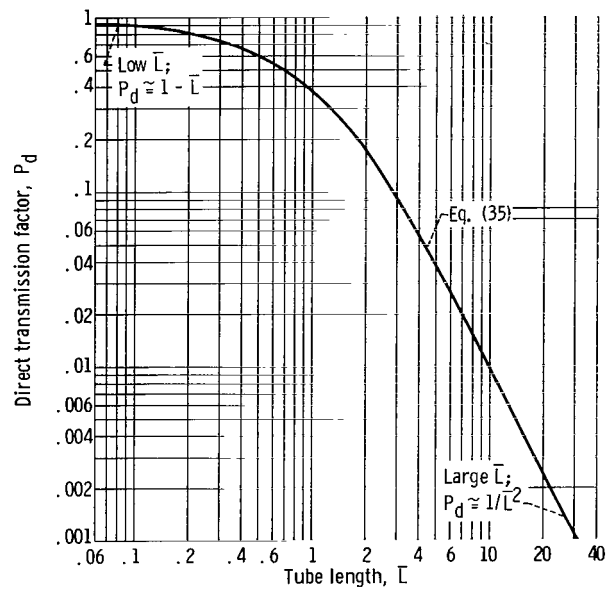

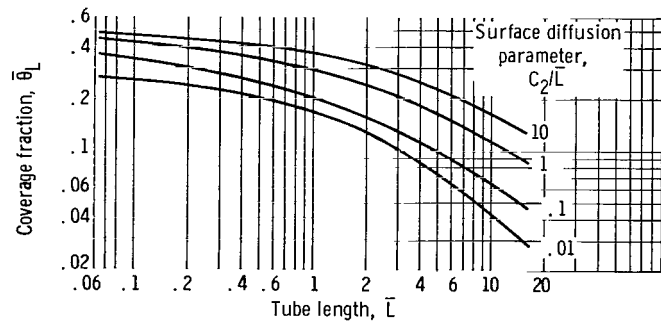Figure 4. - Variation of direct transmission factor with tube length.

Figure 5. – Matched solutions of variation of surface coverage at down-
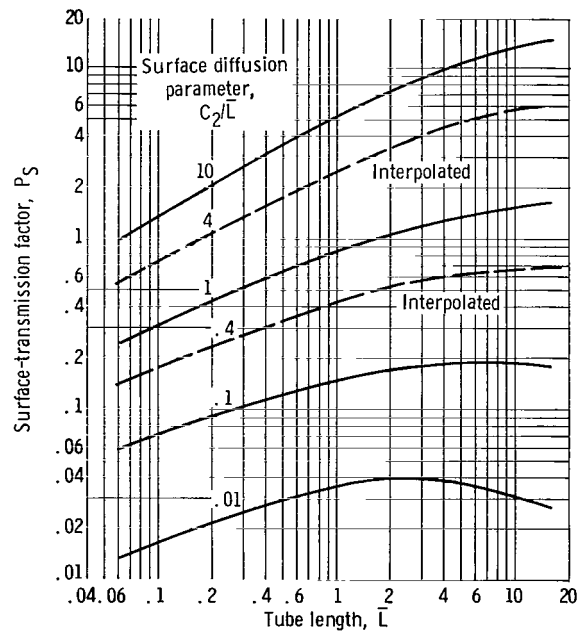stream end of tube with tube length.

Figure 6. – Matched solutions of variation of downstream
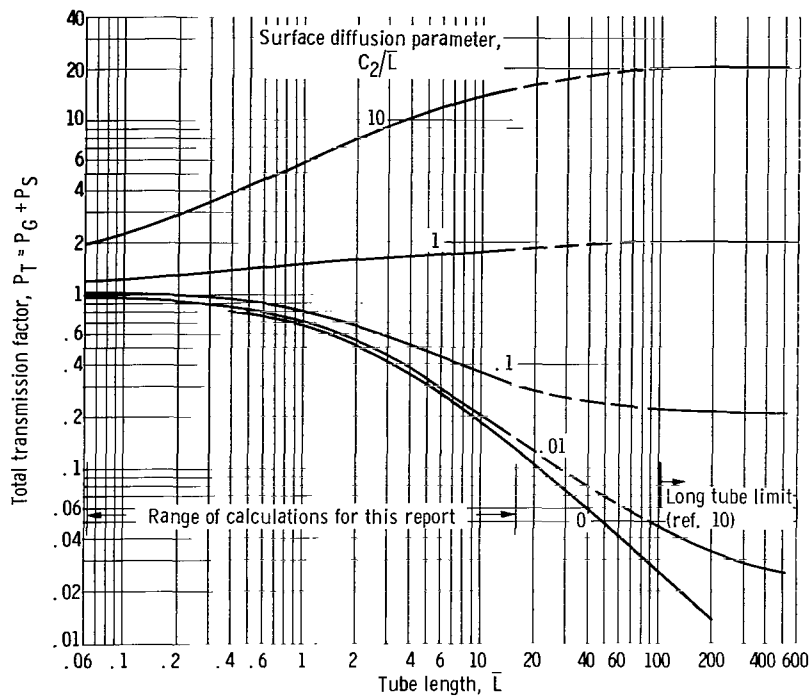surface-transmission factor with tube length.

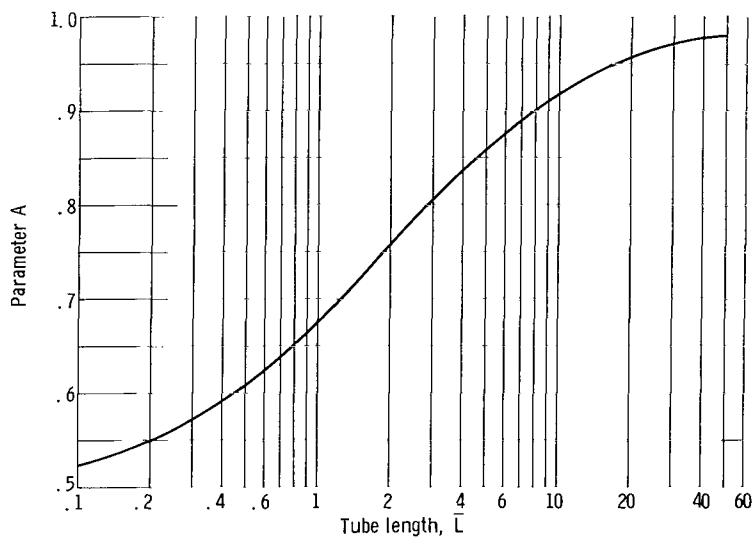Figure 7. – Matched solutions of the variation of total transmission fraction with tube length.

Figure 8. – Variation of parameter A (eq. (B5)) with tube length.

"The aeronautical and space activities of the United States shall be conducted so as to contribute . . . to the expansion of human knowledge of phenomena in the. atmosphere and space. The Administration shall provide for the widest practicable and appropriate dissemination of information concerning its activities and the results thereof."

—NATIONAL AERONAUTICS AND SPACE ACT OF 1958

NASA SCIENTIFIC AND TECHNICAL PUBLICATIONS

TECHNICAL REPORTS: Scientific and technical information considered important, complete, and a lasting contribution to existing knowledge.

TECHNICAL NOTES: Information less broad in scope but nevertheless of importance as a contribution to existing knowledge.

TECHNICAL MEMORANDUMS: Information receiving limited distribution because of preliminary data, security classification, or other reasons.

CONTRACTOR REPORTS: Technical information generated in connection with a NASA contract or grant and released under NASA auspices.

TECHNICAL TRANSLATIONS: Information published in a foreign language considered to merit NASA distribution in English.

TECHNICAL REPRINTS: Information derived from NASA activities and initially published in the form of journal articles.

SPECIAL PUBLICATIONS: Information derived from or of value to NASA activities but not necessarily reporting the results of individual NASA-programmed scientific efforts. Publications include conference proceedings, monographs, data compilations, handbooks, sourcebooks, and special bibliographies.

Details on the availability of these publications may be obtained from:

SCIENTIFIC AND TECHNICAL INFORMATION DIVISION

NATIONAL AERONAUTICS AND SPACE ADMINISTRATION

Washington, D.C. 20546